IL-4 Production by Group 2 Innate Lymphoid cells (ILC2) Promotes Food Allergy by Blocking Regulatory T cell Function

Magali Noval Rivas, PhD,[a,b,§,*], Oliver T. Burton, PhD,[a,b*], Hans C. Oettgen, MD, PhD[a,b,‡] and Talal Chatila, MD, MSc[a,b,‡].

[a]Division of Immunology, Boston Children's Hospital, Boston, MA, USA; [b]Department of Pediatrics, Harvard Medical School, Boston, MA, USA.

[§] Dr. Noval Rivas is currently affiliated with the Division of Pediatric Infectious Diseases and Immunology, Department of Pediatric, Infectious and Immunologic Diseases Research Center, Cedars-Sinai Medical Center, Los Angeles, CA

*****These authors contributed equally to this work.

[‡]These authors contributed equally to this work

Corresponding Author: Talal A. Chatila at the Division of Immunology, Boston Children's Hospital and the Department of Pediatrics, Harvard Medical School.

Address: Karp Family Building, Room 10-214. 1 Blackfan Street, Boston, MA 02115

Email: talal.chatila@childrens.harvard.edu

Methods.

Animals. C.129X1-*Il4ra*$^{tm3.1Tch}$ (*Il4raF709*), C.Cg-*Foxp3*^{tm2Tch}/J (*Foxp3*^{EGFP}) and *DO11.10*$^{+}$*Foxp3*^{EGFP}. *Foxp3*$^{EGFP/DTR+}$, *Foxp3*^{K276x} mice, all BALB/c congenics, were previously described [1-7]. C.129S6(B6)-*Rag2*^{tm1Fwa} (*Rag2*$^{-/-}$) mice were obtained from Taconic and crossed with *DO11.10Foxp3*^{EGFP} and *DO11.10*$^{+}$*Il4raF709 Foxp3*^{EGFP} mice [8]. C.129S4(Cg)-*Il13*$^{tm2.1Lky}$/J (*IL-13YFP*$^{-Cre}$), C.129-*Il4*^{tm1Lky}/J, C.129Ola-*Il13*$^{tm1.1Anjm}$ and BALB/c-*Il4*^{tm2Nnt}/J (*Il4*$^{-/-}$) mice were obtained from the JAX lab and maintained in our animal facility. BALB/c congenic *Il1rl1*$^{-/-}$ mice, a gift from Dr. Andrew McKenzie, were backcrossed with *Il4raF709* mice in order to generate *Il4raF709 Il1rl1*$^{-/-}$ mice [9]. Mice were bred and housed under specific pathogen-free conditions and used according to the guidelines of the Institutional Animal Research Committee at the Boston Children's Hospital of Animal Care Resources.

Flow cytometry. The following murine antibodies were used: CD45 (30-F11), Thy1.1 (HiS51), Thy1.2 (30-H12), CD25 (PC61.5), CD4 (RM4-5), CD3 (145-2C11), IL-17 (TC11-18H10.1), c-Kit (2B8), Sca-1(D7), IL-5 (TRFK5), TCRβ (H57-597, F4/80 (BM2), CD124 (IL-4Rα; I015F8) (Biolegend), Foxp3 (FJK-16S), DO11.10 (KJ126), IL-13 (eBio13a), GATA-3 (TWAJ), ICOS (C398.4A), IFNγ (XMG1.2), RORγt (B2), Rat IgG1 Isotype control (eBRG1), CD213a1 (IL-13Rα; 13MOKA) (eBioscience), ST2 (DJ8) (MD Biosciences), IL-4 (11B11), CD127 (SB/199) (BD Biosciences). Exclusion of lineage marker-expressing cells was accomplished using a cocktail of FITC- or PE-conjugated antibodies comprised of B220 (RA3-6B2), CD3ε (145-2C11), CD4 (RM4-5), CD8α (53-6.7), CD49b (DX5), CD11b (M1/70), CD11c (N418), CD19 (6D5), Gr-1 (RB6-8C5), FcεRIα (MAR-1), NKp46 (29A1.4) and TCRγδ (UC7-13D5) (Biolegend). For cytokines and nuclear factors intracellular staining, cells were stimulated during 4 hours with PMA (50 ng/ml; Sigma-Aldrich) and ionomycin (500

ng/ml; Sigma-Aldrich) in the presence of Golgi Plug (BD Biosciences), stained with the BD Cytofix/Cytoperm buffers (BD Biosciences) or with the Foxp3 Transcription Factor buffer set (eBioscience). Cell proliferation assays were performed with the Violet CellTrace Dye (Invitrogen) as previously described [1]. Dead cells were routinely excluded from the analysis based on the staining of eFluor 780 fixable viability dye (eBioscience), and analyses were restricted to single cells using FSC-H and FSC-W signals. Stained cells were analyzed on an LSRII Fortessa (BD Biosciences) and data were processed using Flowjo (Tree Star Inc.).

TGF-β-mediated *in vitro* iTreg cell induction. Sorted naïve $CD4^+$ T cells ($1x10^6$/ml) were cultured with plate-bound anti-CD28 (5µg/ml, Biolegend), anti-CD3 (1µg/ml, Biolegend), recombinant TGF-β (10ng/ml, R&D Systems), retinoic acid (100nM, Sigma-Aldrich), anti-IFNγ (5µg/ml, XMG1.2, Biolegend), IL-2 (2ng/ml, Shenandoah Biotechnology) and anti-IL-4 (20µg/ml, 11B11, prepared in house). After 7 days, the induced iTreg cells were analyzed by flow cytometry or resorted upon eGFP fluorescence.

Diphtheria toxin Treg cell depletion. For *in vivo* Treg cell depletion, *Foxp3*$^{EGFP/DTR+}$ and control *Foxp3*^{EGFP} mice were given 50 µg/kg of diphtheria toxin (DT, Sigma Aldrich) i.p. every other day during 2 weeks as previously described [6]. Mice were analyzed the following day of the last DT injection and Treg cell depletion was assessed by flow cytometry in the MLN and SI of the treated mice.

Quantitative real-time PCR analysis. Jejunal sections were snap-frozen in liquid nitrogen and homogenized in Trizol (Life Technologies). RNA was extracted from the homogenized tissues by using the RNeasy kit (Qiagen). Reverse transcription was performed using Superscript III and oligo dT (Invitrogen). TaqMan gene probes were

used with TaqMan Universal Fast Master Mix (Applied Biosystems) and ran on a Step-One-Plus machine (Applied Biosystems). *Gapdh* was used as an endogenous control (Applied Biosystems) and WT mouse RNA as the exogenous control. Samples were run in triplicates and the relative expression was calculated using the ΔΔCt method.

ELISAs. Murine mast cell protease 1 (MMCP-1), total and OVA-specific IgE concentrations were measured in the sera of treated mice by ELISAs, as described previously [5]. Peanut-specific IgE was captured onto ELISA coated overnight with 3µg/ml anti-IgE (R35-92, BD) and detected using 200ng/ml biotinylated peanut extract as previously described [2].

Peanut-specific T cell assays. $CD4^+$ T cells from sensitized mice were assessed for peanut-responsiveness as previously described [2]. Briefly, MLN cells were labeled with CellTrace Violet and cultured with aqueous protein extract from peanut flour for 5 days prior to analysis by flow cytometry. Cells undergoing proliferation (dye dilution) in response to stimulation were considered peanut-specific.

Histological analysis. Intestinal mast cells were enumerated by microscopic examination of jejunal sections fixed in 10% formaldehyde and stored in ethanol 70% before toluidine blue staining by the Harvard Rodent Histopathology Facility.

Supplementary Figure Legends.

Figure E1. OVA-sensitization expands ILC2 in *Il4raF709* mice. (A) Core body temperature changes of PBS or OVA/SEB-sensitized WT and *Il4raF709* mice after oral OVA challenge. **(B - C)** Serum levels of total and OVA-specific IgE (B); serum MMCP-1 release and intestinal mast cell numbers after anaphylaxis (C). **(D)** *Il25* and *Il33* mRNA in the SI. **(E - F)** Flow cytometric analysis of ILC2 (Lin^- $Thy1.2^+$ $CD25^+$ $CD127^+$ $Sca\text{-}1^{high}$ $c\text{-}Kit^{low}$) and ILC3 (Lin^- $Thy1.2^+$ $CD25^+$ $CD127^+$ $Sca\text{-}1^-$ $c\text{-}Kit^+$) in the MLN (E) and SI of OVA-SEB sensitized mice (F). **(G - H)** Frequencies and absolute numbers of ILC2 and ILC3 in the SI (G) and MLN (H) of OVA/SEB-sensitized WT and *Il4raF709* mice. Results representative of 2 independent experiments with 5 mice per group. *P < .05, **P < 0.01 and ***P < 0.001 by two-way ANOVA and one-way ANOVA with post-test analysis.

Figure E2. Lin^- $GATA\text{-}3^+$ ILC2 are enriched during food allergy. (A) Flow cytometric gating strategy used to identify ILC2 and ILC3 based on their respective expression of the transcription factors GATA-3 and RORγt. **(B)** Flow cytometric analysis of $GATA\text{-}3^+$ ILC2 and $ROR\gamma t^+$ ILC3 in the MLN and SI of peanut-sensitized WT, *Il1rl1*$^{-/-}$, *Il4raF709* and *Il4raF709 Il1rl1*$^{-/-}$. (**C**) Frequencies and absolute numbers of $GATA\text{-}3^+$ ILC2 and $ROR\gamma t^+$ ILC3 in the MLN and SI of peanut-sensitized WT, *Il1rl1*$^{-/-}$, *Il4raF709* and *Il4raF709 Il1rl1*$^{-/-}$. Results representative of 2 independent experiments, 5 to 8 mice per group. *P < .05, **P < 0.01 and ***P < 0.001 by one-way ANOVA with post-test analysis.

Figure E3. IL-4 expression by ILC2. (A) Flow cytometric analysis of IL-4 production by Lin^- $CD45^+$ $CD25^+$ $CD127^+$ $Sca\text{-}1^{high}$ $c\text{-}Kit^{low}$ ILC2 isolated from the SI *lamina propia* and the MLN of IL-4 eGFP mice based on eGFP expression. (**B**) Detection of

IL-4 signal in TCRβ$^+$ CD4$^+$ T cells, FcεRIα$^+$ c-Kit$^+$ mast cells from the SI *lamina propia* and DX5$^+$ FcεRIα$^+$ c-Kit$^-$ basophils from peripheral blood of IL-4 eGFP mice. **(C)** Flow cytometric analysis of IL-4Rα and IL-13Rα1 expression on F4/80$^+$ CD11b$^+$ macrophages, CD11c$^+$ dendritic cells, TCRβ$^+$ CD4$^+$ T cells, Foxp3$^+$ Treg cells, FcεRIα$^+$ c-Kit$^+$ mast cells and CD19$^+$ B220$^+$ B cells.

Figure E4. *Il1rl1* signaling regulates ILC2 expansion in peanut-sensitized mice. **(A - B)** Flow cytometric analysis of IL-13 and IL-4 (A) and IL-5 and IL-4 (B) expression by intestinal GATA-3$^+$ ILC2 isolated from the SI of PBS- or peanut-sensitized WT, *Il4raF709*, *Il1rl1*$^{-/-}$ and *Il4raF709 Il1rl1*$^{-/-}$ mice. (**C**) Frequencies of IL-4$^+$, IL-5$^+$ and IL-13$^+$ cells among GATA-3$^+$ ILC2 isolated from the SI of PBS- or peanut-sensitized WT, *Il4raF709*, *Il1r1l*$^{-/-}$ and *Il4raF709 Il1rl1*$^{-/-}$ mice. Results represent data on 3 to 6 mice per group derived from 2 independent experiments. *P < .05, **P < 0.01 and ***P < 0.001 by one-way ANOVA with post-test analysis.

Figure E5. Adoptive transfer of *Il13*$^{-/-}$ ILC2 but not ILC3 restores oral sensitization in *Il4raF709 Il1rl1*$^{-/-}$ mice. (A) Core body temperature changes of PBS or peanut-sensitized *Il4raF709 Il1rl1*$^{-/-}$ mice in the absence or after adoptive transfer of *in vitro* WT ILC2 or *Il13*$^{-/-}$ ILC2 or ILC3. (**B**) Serum levels of peanut-specific IgE and MMCP-1 release after anaphylaxis. (**C**) Absolute numbers of GATA-3$^+$ ILC2 and RORγt$^+$ ILC3 from the MLN and SI of PBS or peanut-sensitized *Il4raF709 Il1rl1*$^{-/-}$ mice without or following adoptive transfer of either *in vitro* expanded and cell-sorted WT ILC2, *Il13*$^{-/-}$ ILC2 or ILC3. Data are representative of 4 to 5 mice per group. *P < .05, **P < 0.01 and ***P < 0.001 by two-way ANOVA and one-way ANOVA with post-test analysis.

Figure E6. Impaired allergen-specific iTreg cell induction is permissive to ILC2 expansion. (A - B) Flow cytometric gating strategy used to identify ILC2 ($CD45^+$ $CD4^-$ TCR-β^- Lin^- $Thy1.2^+$ $GATA\text{-}3^+$) and ILC3 ($CD45^+$ $CD4^-$ TCR-β^- $Lin^-$$Th1.2^+$ $ROR\gamma t^+$) in the MLN (A) and SI (B) of WT $DO11.10^+$ $Rag2^{-/-}$ *Foxp3*^{EGFP} and $DO11.10^+$ $Rag2^{-/-}$ *Il4raF709 Foxp3*^{EGFP} mice fed with 1% OVA in drinking water.

Figure E7. Treg cell deficiency in *Foxp3*^{276X} mice results in ILC2 expansion. (A - B) Flow cytometry analysis of Sca-1^{high} c-Kit^{low} ILC2 and Sca-1^- c-Kit^+ ILC3 in the SI (A) and MLN (C) of 21-day-old WT and *Foxp3*^{276X} mice. **(C - D)** Frequencies and absolute numbers of ILC2 and ILC3 in the SI (C) and MLN (D) of 21-day-old WT and *Foxp3*^{276X} mice. Results representative of 2 independent experiments, 3 to 6 mice per group. *P < .05 and**P < 0.01 by unpaired two-tailed Student t test.

Figure E8. *Foxp3*$^{EGFP/DTR+}$ Treg cell depletion following DT administration. (A) Body weight of *Foxp3*^{EGFP} and *Foxp3*$^{EGFP/DTR+}$ mice following 2 weeks of DT treatment. **(B)** Flow cytometric analysis of $CD4^+Foxp3^{EGFP+}$ Treg in the MLN and SI of the mice from (A). **(C)** Frequency and absolute number of $CD4^+Foxp3^{EGFP+}$ Treg cells in the mice from (A). Results representative of 2 independent experiments, 5 mice per group. *P < .05, **P < 0.01 and ***P < 0.001 by unpaired two-tailed Student t test.

References.

1. Noval Rivas M, Burton OT, Wise P, Charbonnier L-M, Georgiev P, Oettgen HC, et al. Regulatory T Cell Reprogramming toward a Th2-Cell- like Lineage Impairs Oral Tolerance and Promotes Food Allergy. Immunity 2015;42:512–23.

2. Burton OT, Noval Rivas M, Zhou JS, Logsdon SL, Darling AR, Koleoglou KJ, et al. Immunoglobulin E Signal Inhibition during Allergen Ingestion Leads to Reversal of Established Food Allergy and Induction of Regulatory T Cells. Immunity 2014;41:141–51.

3. Tachdjian R, Khatib Al S, Schwinglshackl A, Kim HS, Chen A, Blasioli J, et al. In vivo regulation of the allergic response by the IL-4 receptor alpha chain immunoreceptor tyrosine-based inhibitory motif. J Allergy Clin Immunol 2010;125:1128–8.

4. Mathias CB, Hobson SA, Garcia Lloret M, Lawson G, Poddighe D, Freyschmidt E-J, et al. IgE-mediated systemic anaphylaxis and impaired tolerance to food antigens in mice with enhanced IL-4 receptor signaling. J Allergy Clin Immunol 2011;127:795–805.e1–6.

5. Noval Rivas M, Mazmanian S, Burton OT, Wise P, Talal C. A microbiota signature associated with experimental food allergy promotes allergic sensitization and anaphylaxis. 2013;131:201–12.

6. Haribhai D, Williams JB, Jia S, Nickerson D, Schmitt EG, Edwards B, et al. A requisite role for induced regulatory T cells in tolerance based on expanding antigen receptor diversity. Immunity 2011;35:109–22.

7. Haribhai D, Lin W, Edwards B, Ziegelbauer J, Salzman NH, Carlson MR, et al. A central role for induced regulatory T cells in tolerance induction in experimental colitis. J Immunol 2009;182:3461–8.

8. Shinkai Y, Rathbun G, Lam KP, Oltz EM, Stewart V, Mendelsohn M, et al. RAG-2-deficient mice lack mature lymphocytes owing to inability to initiate V(D)J rearrangement. Cell 1992;68:855–67.

9. Townsend MJ, Fallon PG, Matthews DJ, Jolin HE, McKenzie AN. T1/ST2-deficient mice demonstrate the importance of T1/ST2 in developing primary T helper cell type 2 responses. Journal of Experimental Medicine 2000;191:1069–76.

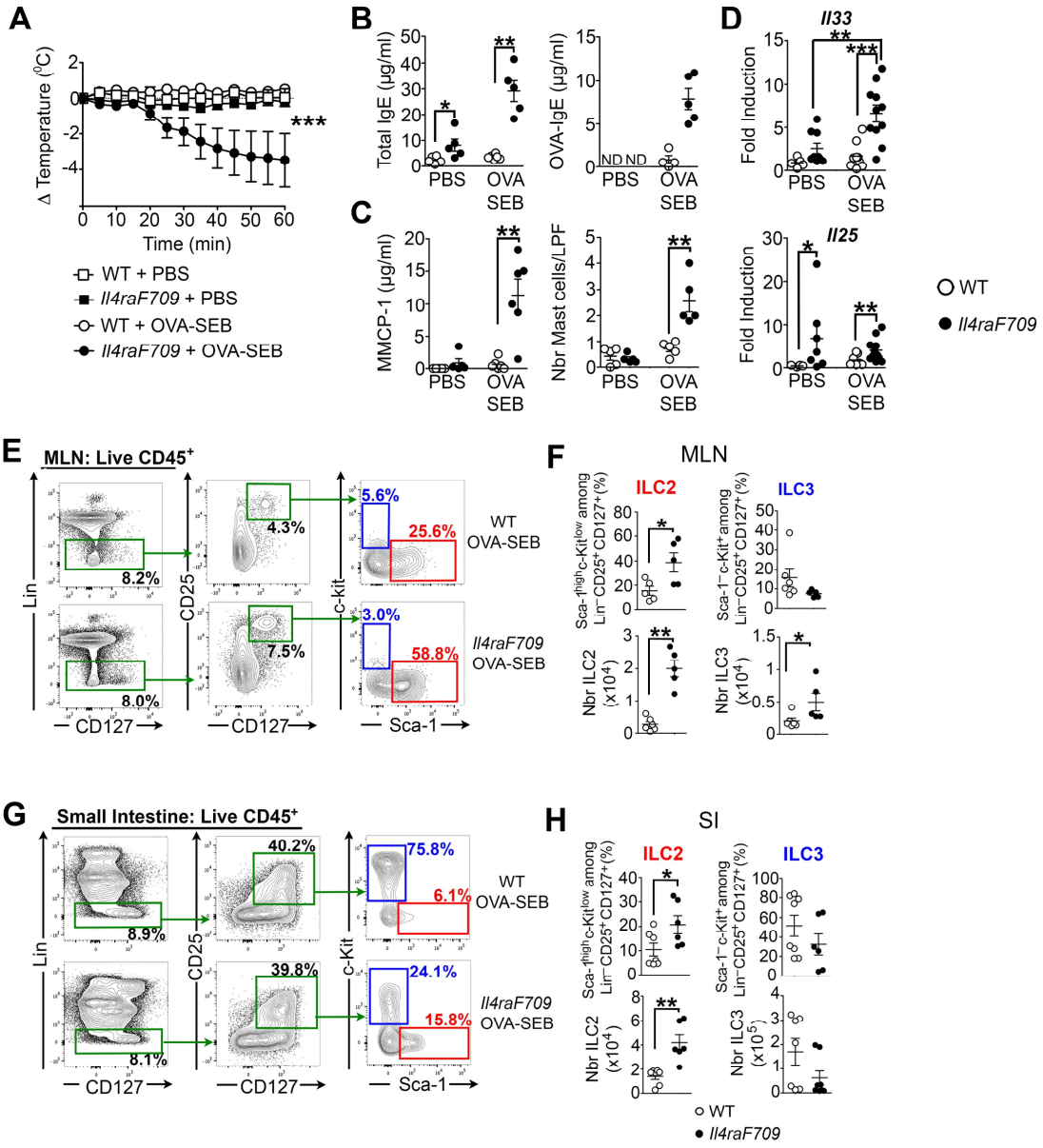
A
Δ Temperature (°C)
Time (min)
WT + PBS
Il4raF709 + PBS
WT + OVA-SEB
Il4raF709 + OVA-SEB
B
Total IgE (μg/ml)
OVA-IgE (μg/ml)
ND ND
PBS
OVA SEB
C
MMCP-1 (μg/ml)
Nbr Mast cells/LPF
D
Il33
Il25
Fold Induction
WT
Il4raF709
E
MLN: Live CD45+
Lin
CD25
c-kit
CD127
Sca-1
8.2%
8.0%
4.3%
7.5%
5.6%
25.6%
3.0%
58.8%
WT OVA-SEB
Il4raF709 OVA-SEB
F
MLN
ILC2
ILC3
Sca-1high c-Kitlow among Lin− CD25+ CD127+ (%)
Sca-1− c-Kit+ among Lin− CD25+ CD127+ (%)
Nbr ILC2 (x10^4)
Nbr ILC3 (x10^4)
G
Small Intestine: Live CD45+
8.9%
8.1%
40.2%
39.8%
75.8%
6.1%
24.1%
15.8%
H
SI
Nbr ILC3 (x10^5)

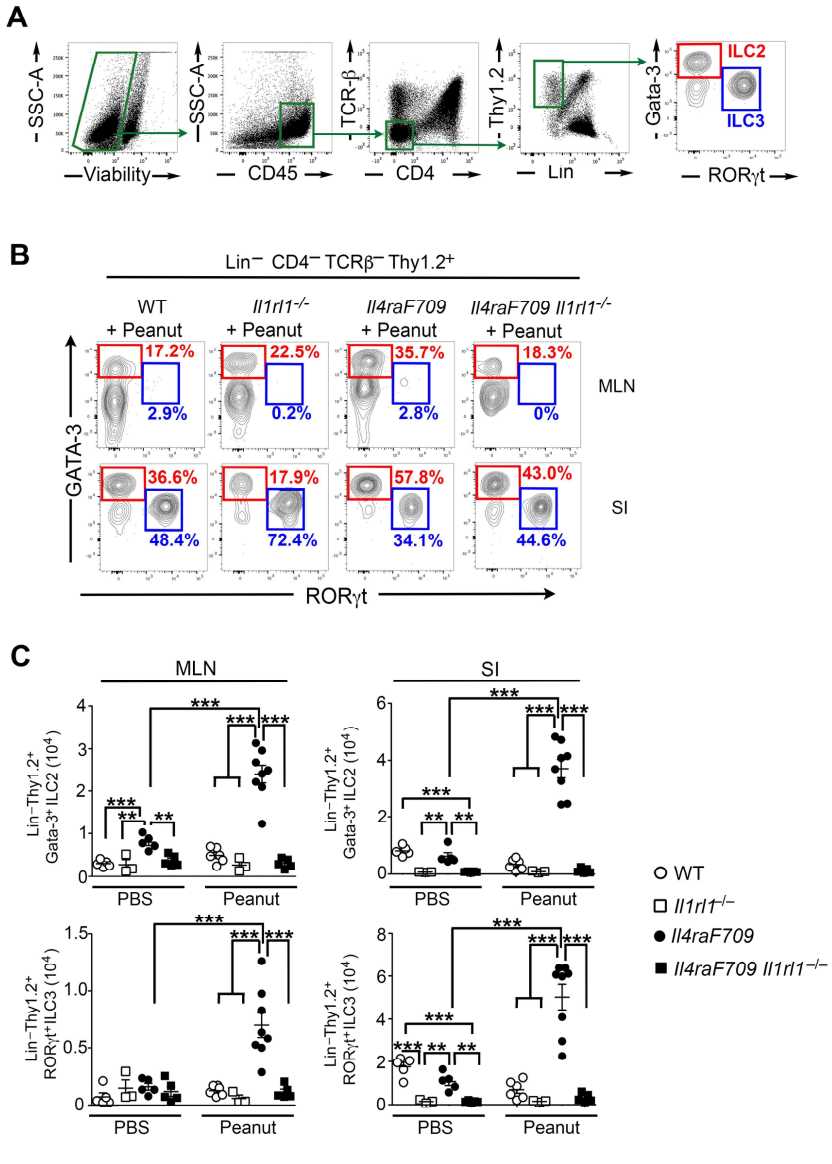
A
SSC-A
Viability
SSC-A
CD45
TCR-β
CD4
Thy1.2
Lin
Gata-3
RORγt
ILC2
ILC3
B
Lin⁻ CD4⁻ TCRβ⁻ Thy1.2⁺
WT + Peanut
Il1rl1-/- + Peanut
Il4raF709 + Peanut
Il4raF709 Il1rl1-/- + Peanut
17.2%
2.9%
22.5%
0.2%
35.7%
2.8%
18.3%
0%
36.6%
48.4%
17.9%
72.4%
57.8%
34.1%
43.0%
44.6%
MLN
SI
GATA-3
RORγt
C
MLN
SI
Lin⁻Thy1.2⁺ Gata-3⁺ ILC2 (10⁴)
Lin⁻Thy1.2⁺ RORγt⁺ILC3 (10⁴)
PBS
Peanut
WT
Il1rl1-/-
Il4raF709
Il4raF709 Il1rl1-/-

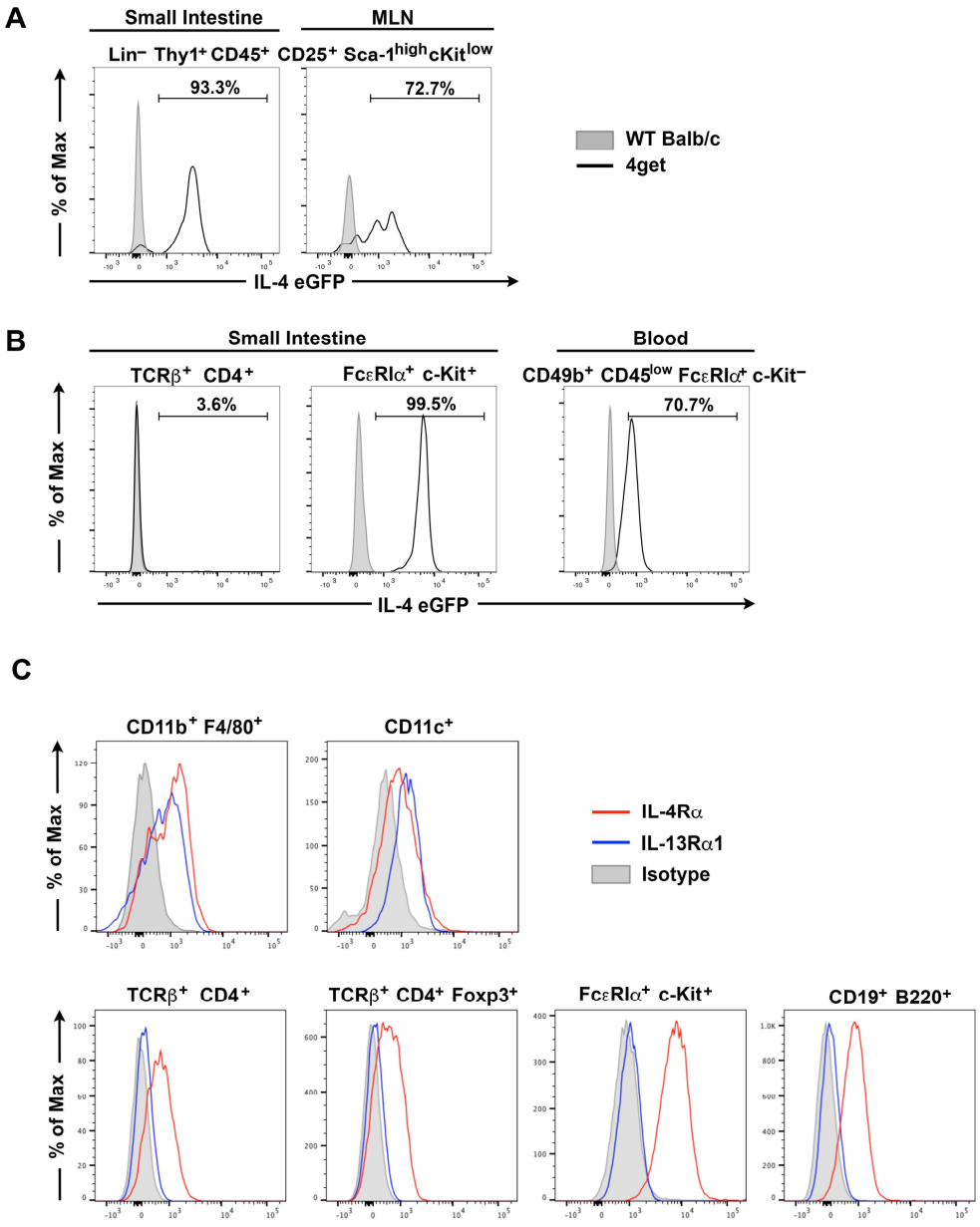
A
Small Intestine
MLN
Lin⁻ Thy1⁺ CD45⁺ CD25⁺ Sca-1^high cKit^low
93.3%
72.7%
% of Max
IL-4 eGFP
WT Balb/c
4get
B
Small Intestine
Blood
TCRβ⁺ CD4⁺
FcεRIα⁺ c-Kit⁺
CD49b⁺ CD45^low FcεRIα⁺ c-Kit⁻
3.6%
99.5%
70.7%
% of Max
IL-4 eGFP
C
CD11b⁺ F4/80⁺
CD11c⁺
% of Max
IL-4Rα
IL-13Rα1
Isotype
TCRβ⁺ CD4⁺
TCRβ⁺ CD4⁺ Foxp3⁺
FcεRIα⁺ c-Kit⁺
CD19⁺ B220⁺
% of Max

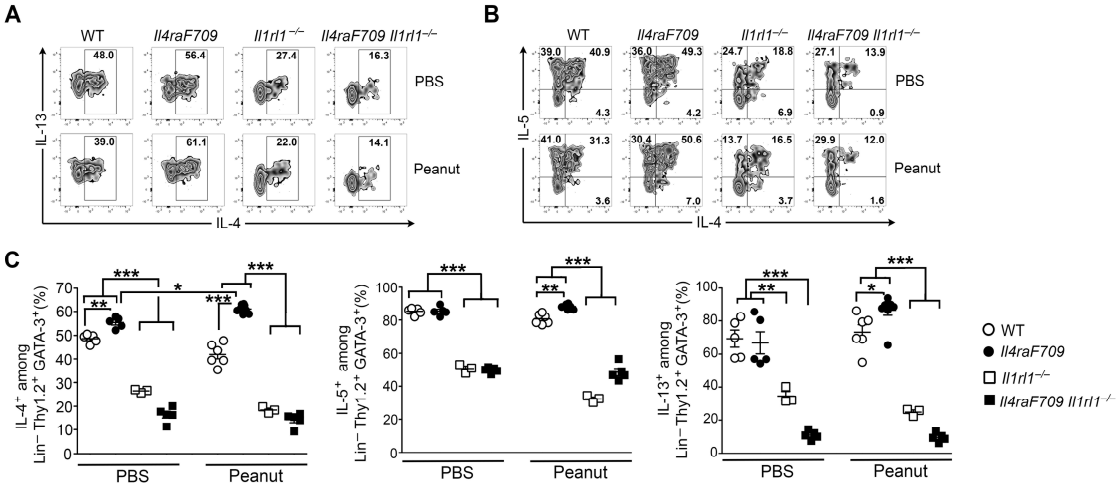
A
WT
Il4raF709
Il1rl1−/−
Il4raF709 Il1rl1−/−
48.0
56.4
27.4
16.3
PBS
39.0
61.1
22.0
14.1
Peanut
IL-13
IL-4
B
WT
Il4raF709
Il1rl1−/−
Il4raF709 Il1rl1−/−
39.0
40.9
4.3
36.0
49.3
4.2
24.7
18.8
6.9
27.1
13.9
0.9
PBS
41.0
31.3
3.6
30.4
50.6
7.0
13.7
16.5
3.7
29.9
12.0
1.6
Peanut
IL-5
IL-4
C
IL-4+ among Lin− Thy1.2+ GATA-3+(%)
IL-5+ among Lin− Thy1.2+ GATA-3+(%)
IL-13+ among Lin− Thy1.2+ GATA-3+(%)
PBS
Peanut
WT
Il4raF709
Il1rl1−/−
Il4raF709 Il1rl1−/−

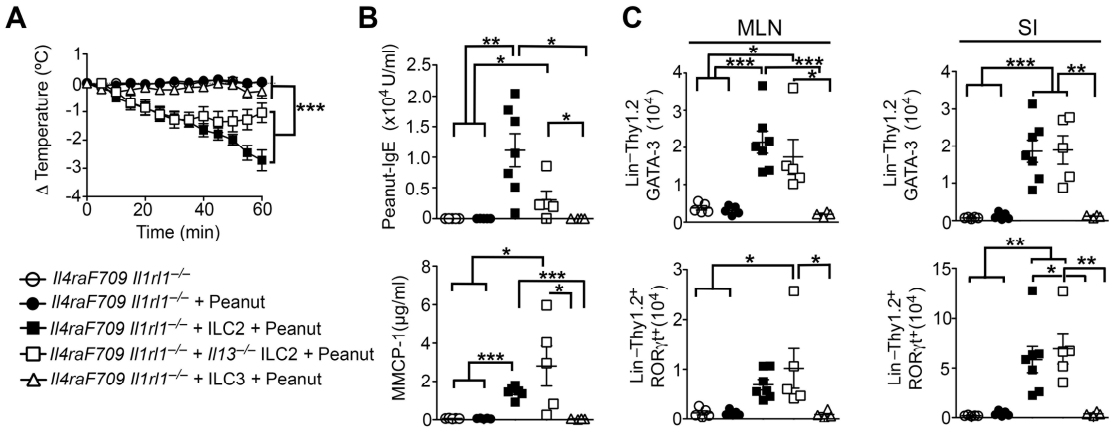
A
B
C
MLN
SI
Δ Temperature (°C)
Time (min)
***
Il4raF709 Il1rl1−/−
Il4raF709 Il1rl1−/− + Peanut
Il4raF709 Il1rl1−/− + ILC2 + Peanut
Il4raF709 Il1rl1−/− + Il13−/− ILC2 + Peanut
Il4raF709 Il1rl1−/− + ILC3 + Peanut
Peanut-IgE (x10⁴ U/ml)
MMCP-1(μg/ml)
Lin−Thy1.2 GATA-3 (10⁴)
Lin−Thy1.2+ RORγt+(10⁴)

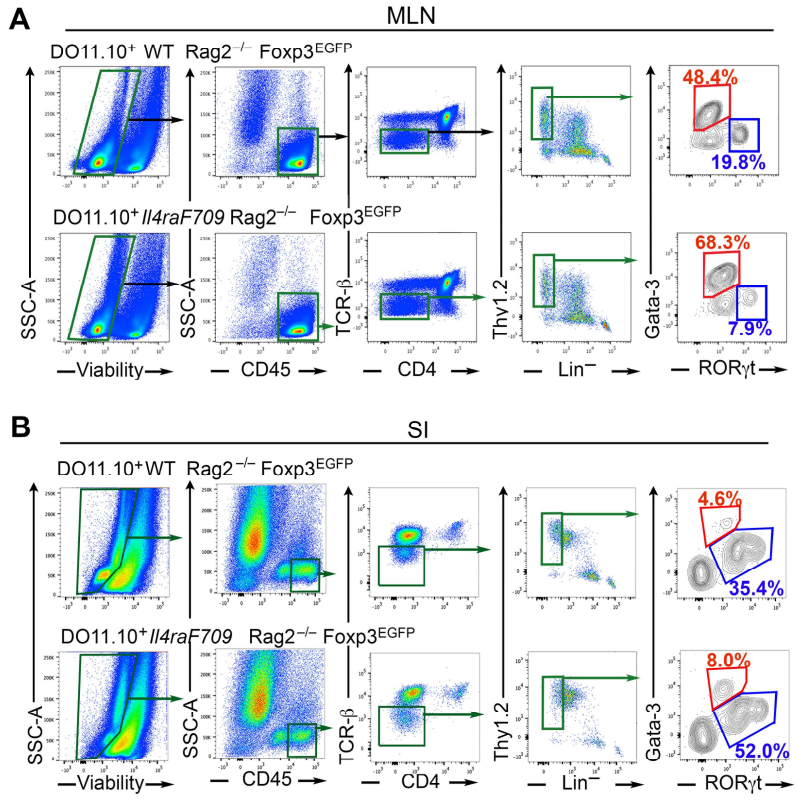
A
MLN
DO11.10+ WT Rag2−/− Foxp3EGFP
DO11.10+ Il4raF709 Rag2−/− Foxp3EGFP
48.4%
19.8%
68.3%
7.9%
SSC-A
Viability
CD45
TCR-β
CD4
Thy1.2
Lin−
Gata-3
RORγt
B
SI
DO11.10+WT Rag2−/− Foxp3EGFP
DO11.10+ Il4raF709 Rag2−/− Foxp3EGFP
4.6%
35.4%
8.0%
52.0%

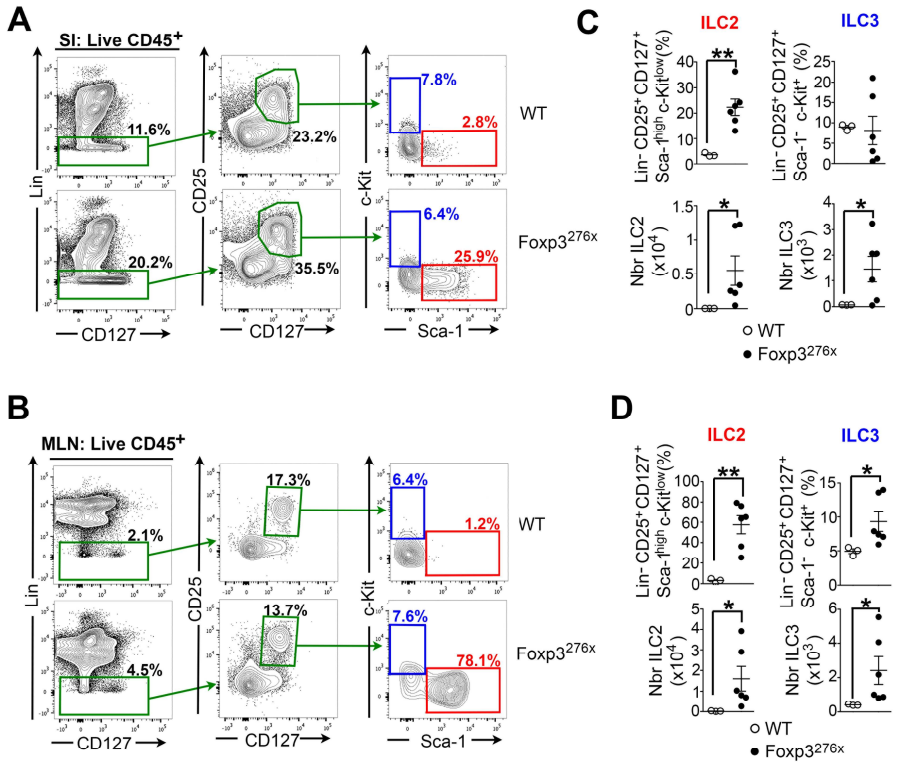
A
SI: Live CD45+
11.6%
20.2%
23.2%
35.5%
7.8%
2.8%
6.4%
25.9%
WT
Foxp3276x
Lin
CD25
c-Kit
CD127
CD127
Sca-1
B
MLN: Live CD45+
2.1%
4.5%
17.3%
13.7%
6.4%
1.2%
7.6%
78.1%
WT
Foxp3276x
Lin
CD25
c-Kit
CD127
CD127
Sca-1
C
ILC2
ILC3
Lin- CD25+ CD127+ Sca-1high c-Kitlow (%)
Lin- CD25+ CD127+ Sca-1- c-Kit+ (%)
Nbr ILC2 (x10^4)
Nbr ILC3 (x10^3)
**
*
*
WT
Foxp3276x
D
ILC2
ILC3
Lin- CD25+ CD127+ Sca-1high c-Kitlow (%)
Lin- CD25+ CD127+ Sca-1- c-Kit+ (%)
Nbr ILC2 (x10^4)
Nbr ILC3 (x10^3)
**
*
*
*
WT
Foxp3276x

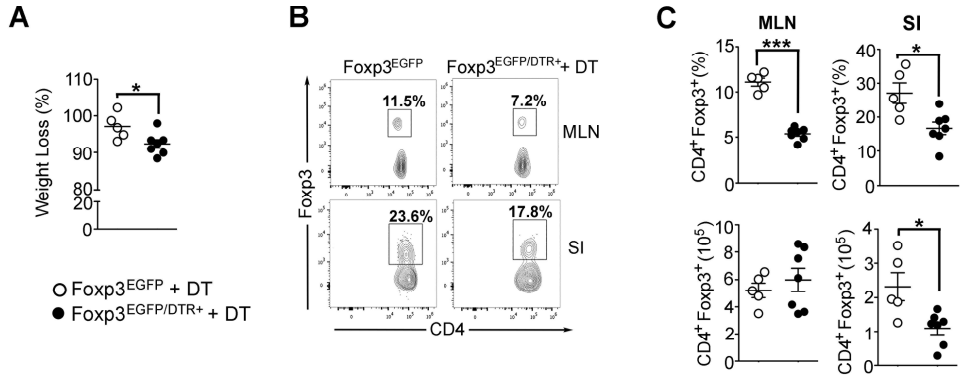
A
B
C
Weight Loss (%)
110
100
90
80
20
0
*
Foxp3EGFP + DT
Foxp3EGFP/DTR+ + DT
Foxp3EGFP
Foxp3EGFP/DTR+ + DT
11.5%
7.2%
23.6%
17.8%
MLN
SI
Foxp3
CD4
MLN
SI
***
*
CD4+ Foxp3+ (%)
CD4+ Foxp3+ (10^5)